Structural, Kinetic, and Mechanistic Aspects of Cation Complexation by *cyclo*-(L-Pro-L-Val-D-Ala-D-Val)$_3$

D. G. Davis*[1a] and B. F. Gisin[1b]

Contribution from the Department of Chemistry, Adelphi University, Garden City, New York 11530, and the Department of Biochemistry, The Rockefeller University, New York, New York 10021. *Received December 6, 1978*

Abstract: Proton nuclear magnetic resonance studies were carried out on *cyclo*-(L-Pro-L-Val-D-Ala-D-Val)$_3$ (PVAV), a synthetic peptide analogue of the ion transport antibiotic valinomycin. For both the free and cation-complexed forms all resonances were assigned unambiguously, including those of the D- and L-valines where nuclear Overhauser enhancement techniques were used. The latter approach also provided an estimate of the relative internuclear distances between non-spin-coupled proton pairs. In the cation complexes, the peptide backbone is folded into six alternating, hydrogen-bonded, type II β(1←4) turns ($\phi_2^{\text{L-Val}} = -65°$; $\phi_2^{\text{D-Val}} = +70°$; $\phi_3^{\text{D-Ala}} = +88°$) and has approximate S_6 symmetry. The cation is located inside a distorted octahedral cavity formed by the carbonyl oxygens of the valines. The uncomplexed form has C_3 symmetry. Its conformation differs from that of the complexes in that the β turns formed by the L-Pro-L-Val-D-Ala-D-Val segments are disrupted, while the D-Ala-D-Val-L-Pro-L-Val β turns remain intact ($\phi^{\text{L-Val}} = -69°$; $\phi^{\text{D-Val}} = +91°$; $\phi^{\text{D-Ala}} = 85°$). Consequently, the entrance to the cation binding site on the proline–valine side is enlarged to provide a pathway for the capture and release of cations. The rate of the peptide–cation dissociation reaction in methanol is slow ($k_d = 4 \times 10^{-4}$ s^{-1}). It was determined by a novel technique based on deuterium exchange between amides and solvent in mixtures of K^+-PVAV and PVAV.

Introduction

Valinomycin (VAL), first described by Brockmann[2] and synthesyzed by Shemyakin,[3] is a cyclic dodecadepsipeptide antibiotic that drastically alters the ionic permeability of natural[4] and artificial[5] lipid membranes. This effect was recognized to be based on the ability of VAL to form, with high selectivity, a hydrophobic inclusion complex with the potassium ion and to transport it through the membrane.[6] Analysis by X-ray diffraction[7] and NMR spectroscopy[8] showed the cation sitting inside the macrocycle, symmetrically surrounded by the six ester carbonyl groups. All of the side chains (methyl and isopropyl groups) are located on the surface and all of the peptide groups form intramolecular hydrogen bonds. This uniquely symmetrical structure has been investigated further in great detail[6,9,10] as a simple model for biological inclusion complexes of a more intricate nature.

Synthetic efforts designed to further our understanding of the mode of action of ionophores have yielded a large number of depsipeptide[11,12] and several peptide[13-16] analogues. The latter, lacking α-hydroxy acid residues entirely, exhibit ion transport properties that are strikingly different from those of their natural counterpart. For instance, the peptide *cyclo*-(L-Pro-L-Val-D-Pro-D-Val)$_3$, PV,[13] has a 10^4 times greater affinity for K^+ than VAL, yet it is 10^3 times less potent in mediating ion transport across lipid bilayer membranes.[17] Similarly, *cyclo*-(L-Pro-L-Val-D-Ala-D-Val)$_3$, PVAV,[18] binds the alkali cations ten times stronger than VAL but it has almost no effect on membranes.

VAL	*cyclo*-(L-Lac-L-Val-D-Hyv-D-Val)$_3$
PV	*cyclo*-(L-Pro-L-Val-D-Pro-D-Val)$_3$
PVAV	*cyclo*-(L-Pro-L-Val-D-Ala-D-Val)$_3$

Clearly, changes in the primary structure of these compounds give rise to differences in their functional properties that are not predictable from the study of their covalent structures or molecular models. However, they may now be understood based on results obtained by electrical relaxation techniques on lipid membranes. Thus, it was shown that PV acts predominantly by a carrier mechanism in which the cation is bound in the aqueous phase (solution complexation) whereupon the complex crosses the membrane just like a large hydrophobic ion.[19] In contrast, VAL binds the cation in one water–membrane interface (interfacial complexation) and releases it on the other for a much more efficient mechanism of ion transport.[20] PVAV, it was argued,[18] would be ineffective as an ion carrier because it has too low an aqueous cation binding constant to use the solution complexation mechanism and too slow dissociation kinetics to use the interfacial complexation mechanism.

Evidence to support this hypothesis can be obtained from ^{1}H nuclear magnetic resonance (NMR) studies. In this contribution a detailed NMR analysis of PVAV and its monovalent cation complexes is presented. The dissociation rate of the K^+-PVAV complex was determined by a novel technique and found to be very slow. Furthermore, evidence was obtained to support the notion that there is a preferred pathway for the cation to enter and leave the binding site.

Experimental Section

Materials. The synthesis of PVAV is described elsewhere.[18] Alkali-metal ion and NH_4^+ complexes of PVAV were prepared by adding crystals of the appropriate 2,4,6-trinitro-*m*-cresolate (TNC) salt to a chloroform solution of the free peptide (ca. 1×10^{-3} M). Owing to their low solubility in chloroform (ca. 1×10^{-4} M) the complexes crystallized out of solution as they were formed. The crystals were collected, dried, and dissolved in methylene chloride-d_2. Any residue and unreacted (insoluble) salt was removed by filtration through glass wool. Tetramethylsilane (Me_4Si) was added as an internal frequency reference.

All other materials and solvents were obtained from commercial sources and were used without further purification. Acetone-d_6 and acetonitrile-d_3 (Stohler Isotopes) were stored over molecular sieves to remove traces of water.

Methods. ^{1}H NMR spectra were recorded using two different spectrometers. The one, a Varian 220-MHz spectrometer, was equipped with a Nicolet 1080 accessory and operated in the Fourier transform (FT) mode; the other, an MPC 250-MHz spectrometer (CMU Facility for Biomedical Research), was operated in the correlation mode.[21,22] Variable-temperature experiments at 220 MHz utilized the accessory provided with the instrument. Probe temperatures were determined using standard, precalibrated samples of ethylene glycol before and after recording each spectrum of interest.

Double-resonance difference spectra were taken at 250 MHz as described previously.[23] The power of the second irradiating field, H_2, was generally set at a level just sufficient to "tickle" transitions that are spin coupled to the perturbed (H_2-irradiated) states. To minimize Block–Siegert shifts,[24] the frequency of H_2 used in recording the "unperturbed" spectra was offset ca. 50 Hz from that used in recording the perturbed spectra. Nuclear Overhauser effects[25,26] (NOEs) were measured by taking the ratio of the integrated intensities

0002-7863/79/1501-3755$01.00/0

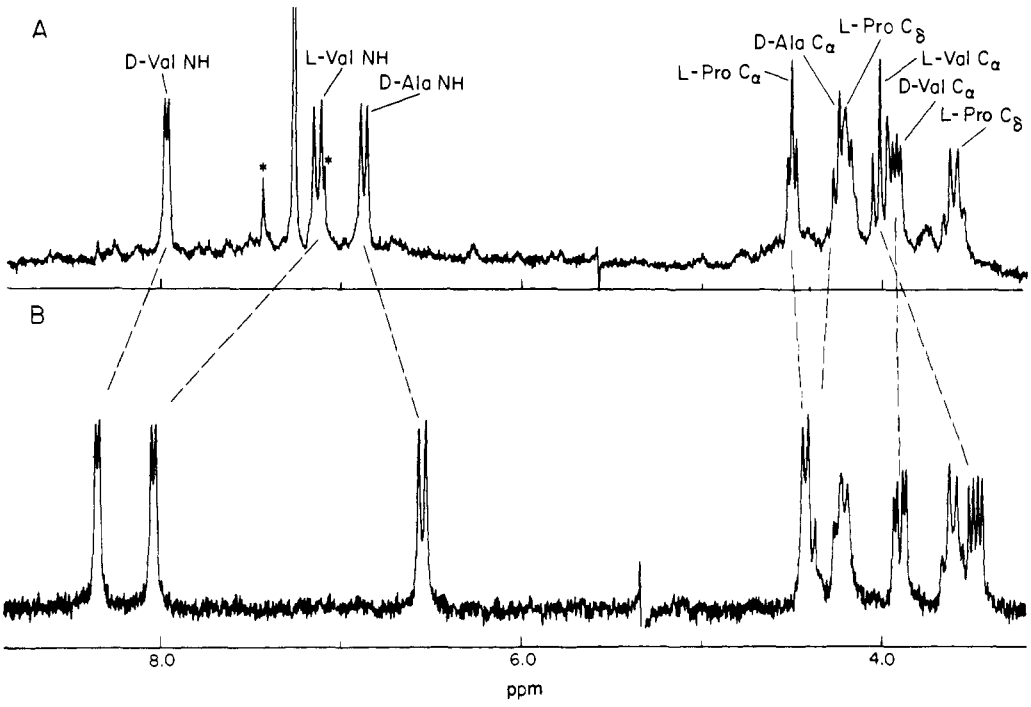

Figure 1. 220-MHz ^1H NMR spectra of free and complexed PVAV. (A) Free PVAV in chloroform-d_1. (B) K^+-PVAV in methylene chloride-d_2. Only the low-field portions of the spectra are shown. Chemical shifts are given relative to Me_4Si. Peptide concentrations are ca. 2×10^{-3} M.

of the lines showing NOEs in the difference spectra to the intensities of the same lines in the unperturbed spectra.

Results

A. ^1H NMR Spectra of Uncomplexed PVAV. A portion of the 220-MHz NMR spectrum of PVAV in chloroform-d_1, showing the resonance of the peptide backbone protons, N-H and C_α-H, and the C_δ-H protons of the proline ring is depicted in Figure 1A. The chemical shifts and coupling constants (including values for some lines not shown in Figure 1) are given in Tables I and II. Most of the resonances could be assigned using standard techniques including double-resonance methods. The latter technique was also used to determine nuclear Overhauser enhancement factors.[26] As described in section C, such data allowed the amide and C_α proton resonances of the D- and L-valine residues to be assigned unambiguously. Since single-resonance lines are observed for all chemically equivalent protons it is concluded that on the NMR time scale the conformation of PVAV in chloroform reflects the C_3 symmetry inherent in its covalent structure.

Solvent accessibility and hydrogen-bonding patterns of the amide protons were determined using variable-temperature, isotope exchange, and solvent perturbation techniques.[27] The temperature studies showed that the low-field, D-valine N-H doublet has a temperature coefficient of 10^{-2} ppm/°C, whereas the high-field L-valine and D-alanine N-H doublets have coefficients of 1 and 3×10^{-3} ppm/°C, respectively. Other portions of the spectra did not change over the range of temperature studied (25-45 °C). Isotope exchange experiments showed that, immediately after a small amount of methanol-d_4 was added to a chloroform solution of PVAV, the D-valine and D-alanine amide proton lines lost intensity (by ^1H-^2H exchange) at similar rates ($t_{1/2}$ ca. 30 min in 0.1% methanol-d_4 at t = 23 °C). In contrast, there was no decrease in the intensity of the L-valine amide proton resonance over the same time course. When small amounts of acetone were added to chloroform solutions of PVAV, the alanine N-H line shifted to lower field while the positions of the D- and L-valine N-H lines were virtually unaffected (Figure 2).

These results indicate that the D-alanine amide protons are exposed to the solvent, while those of L-valine are shielded from the solvent. The slow rate of exchange, coupled with its low temperature coefficients, further suggests that the shielding of the L-valine amide protons is due to intramolecular H bonding. The status of the amide protons of D-valine is more problematic. Although it is not significantly perturbed by the H-bond acceptor acetone, it does exchange with ^2H at a rate comparable to that of the free alanine N-H. Judging from its higher temperature coefficient it might therefore best be characterized as a group which either oscillates readily between a weak intramolecularly H-bonded state and a solvent-exposed state, or is subject to peptide-peptide interactions.

When the mole fraction of acetone in a chloroform solution of free PVAV exceeded 30%, a new series of lines appeared and grew in intensity as the mole fraction of acetone was increased. These new lines correspond to a second conformer that is asymmetric and in equilibrium with the original one. As shown in Figure 3A, at least eight new lines can be identified in the amide region of the PVAV spectra in pure acetone. (Similar spectra are also observed in acetonitrile and methanol.) Within experimental error these lines are all of equal intensity and account for ca. 60% of the total. The remaining 40% can be assigned to the three amide protons of a C_3-symmetric conformer similar to the one observed initially in pure chloroform and in the chloroform-acetone mixtures. New lines also appear in other regions of the spectra but they are generally too poorly resolved for accurate analysis. The alanine methyl resonances are, however, clearly split into one major doublet (40%) and three smaller doublets (60%) of equal intensity (Figure 3B).[28]

B. ^1H NMR Spectra of the Cation Complexes of PVAV. The 220-MHz spectrum of the peptide backbone protons of the K^+-PVAV complex in methylene chloride-d_2 is shown in Figure 1B.This spectrum is generally representative of all the monovalent cation complexes studied including those of Li^+, Na^+, Rb^+, Cs^+, and NH_4^+ (Tables I and II). Clearly, the spectra and properties of the complexes differ from those of free PVAV in several ways. Upon complex formation all protons of the backbone (except $C_\alpha^{L\text{-}Pro}$ and $C_\alpha^{L\text{-}Val}$) shift by approximately ±0.5 ppm (Table I). At the same time the

Table I. Chemical Shifts[a] for PVAV[b] and Its Cation Complexes[c]

compd	D,L-valine					D-alanine			L-proline		
	N^L	$C_\alpha{}^L$	N^D	$C_\alpha{}^D$	$C_{\beta\gamma}{}^{DL}$	N	C_α	C_β	C_α	$C_{\delta,\delta'}$	$C_{\beta,\gamma}$
free	7.13 (10^{-3})[d]	3.93	7.90 (10^{-2})[d]	4.00	1.98 (β) 1.05 (γ) 0.97 (γ) 0.85 (γ) 0.90 (γ)	6.86 (3×10^{-3})[d]	4.22	1.47	4.19	4.19 3.59	1.98
Li^+	7.46		7.67			6.90	4.60		4.39	4.20 3.58	
Na^+	7.47	3.57	7.56	3.90	2.08 (β) 1.11 (γ) 1.07 (γ) 0.95 (γ) 0.94 (γ)	6.92	4.60	1.38	4.39	4.20 3.58	2.08
K^+	8.02	3.45	8.34	3.88	2.06 (β) 1.16 (γ) 1.13 (γ) 0.96 (2)	6.53	4.39	1.40	4.41	4.20 3.57	2.06
Rb^+	7.89	3.42	8.21	3.85	2.05 (β) 1.15 (γ) 1.12 (γ) 0.95 (2)	6.53	4.41	1.40	4.40	4.21 3.58	2.05
Cs^+	7.70	3.40	7.98	3.84	2.05 (β) 1.14 (γ) 1.10 (γ) 0.945 (γ) 0.916 (γ)	6.57	4.53	1.39	4.38	4.20 3.56	2.06
NH_4^+	7.87	3.42	8.16	3.87	2.06 (β) 1.15 (γ) 1.11 (γ) 0.950 (γ) 0.945 (γ)	6.53	4.52	1.39	4.39	4.20 3.58	2.06

[a] In parts per million (±0.005) from Me_4Si. [b] In chloroform-d_1 (2×10^{-3} M); t = 23 °C. [c] In methylene chloride-d_2 ($1-2 \times 10^{-3}$ M); t = 23 °C. [d] Temperature coefficient (ppm/°C).

Table II. Vicinal Coupling Constants[a] and Torsional Angles[b] for PVAV and Its Cation Complexes

	L-Val				D-Val				D-Ala		
	J_{NC_α}	ϕ_2	$J_{C_\alpha C_\beta}$	χ^e	J_{NC_α}	ϕ_2	$J_{C_\alpha C_\beta}$	χ^e	J_{NC_α}	ϕ_3	$J_{C_\alpha C_\beta}$
free PVAV[c]	5.0	−69	9.8	152 (0.75)	8.7	91	8.5	145 (0.60)	7.9	+85	6.8
K^+, Rb^+, Cs^+, NH_4^+-PVAV[d]	4.1	−65	10.9	162 (0.88)	5.2	70	11.2	166 (0.91)	8.3	+88	7.4
Na^+, Li^+-PVAV[d]	4.3	−66	9.8	152 (0.75)	6.3	76	10.6	160 (0.85)	8.8	+91	7.4

[a] In hertz (±0.2). [b] Torsional angles ϕ and χ (deg) are calculated from J_{NC} and $J_{C_\alpha C_\beta}$, respectively, using equations given by Bystrov (ref 29). The designation of ϕ and χ is according to the 1970 IUPAC convention.[44] No corrections for the electronegativity of the substituents on C_α were made. [c] In chloroform-d_1 (t = 23 °C). [d] In methylene chloride-d_2 (t = 23 °C). [e] Value for χ is for nonclassical rotamer configuration; quantity in ( ) is the fraction of trans rotamer derived from averaging over classical rotamer populations according to Pachler (ref 45).

NH-C_αH vicinal coupling constants (J_{NC_α}) change. The values of the torsional angles ϕ calculated from J_{NC_α}[29,30] indicate that large conformational changes in the peptide backbone have occurred (Table II).

The chemical shifts and coupling constants of the complexes show little or no change in going from methylene chloride to acetone or methanol. Thus, complex formation stabilizes the peptide backbone against distortion by H-bonding solvents. Temperature dependence and ^2H-exchange experiments also suggest tight hydrogen bonding in the cation complexes. The D- and L-valine amide protons have small, nearly identical temperature coefficients ($<10^{-3}$ ppm/°C) and neither set of protons shows any measurable exchange with ^2H, even in pure methanol-d_4, after several days. On the other hand, the alanine amide protons still exchange as rapidly as in the free form.

It is concluded that the cation complexes have two distinguishable features: (1) both the D- and the L-valine amide protons are involved in tight intramolecular H bonds and (2) the D- and L-valyl segments of the peptide backbone are approximately related by inversion symmetry.

C. Nuclear Overhauser Effects. In the course of taking double resonance difference spectra, nuclear Overhauser effects (NOEs)[25,26] were observed for certain lines that were not J-coupled to the irradiated transitions. (The NOEs were positive and appear as residual intensity on the decoupled side of the difference spectra.) As can be seen in Figure 4, irradiation of the alanine amide lines at 1647 (K^+-PVAV) or at 1718 Hz (free PVAV) shows, in addition to the collapse of the directly coupled $C_\alpha{}^{Ala}$-H multiplet to a quartet, a clear increase in the intensities of the noncoupled, high-field $C_\alpha{}^{Val}$-H lines centered at 866 (K^+-PVAV, Figure 4F) and 1000 Hz (free PVAV, Figure 4B). For K^+-PVAV, the NOE factor, $f_{C_\alpha H}(NH)$, is ca. 6 ± 1%. Moreover, the effect is reciprocal: irradiation of the $C_\alpha{}^{VAL}$-H line at 866 Hz also gives a $f_{NH}(C_\alpha H)$ of ca. 6% for the noncoupled N^{Ala}-H transition centered at 1697 Hz. The NOE factor for the $C_\alpha{}^{VAL}$ transition in free PVAV is less than in K^+-PVAV, namely, only ca. 3 ± 1%. Smaller but nonetheless reproducible enhancements of the $C_\alpha{}^{Ala}$-H resonance (ca. 1-2%) are also observed upon irradiation of the low-field N^{Val}-H lines at 2088 (K^+-PVAV,

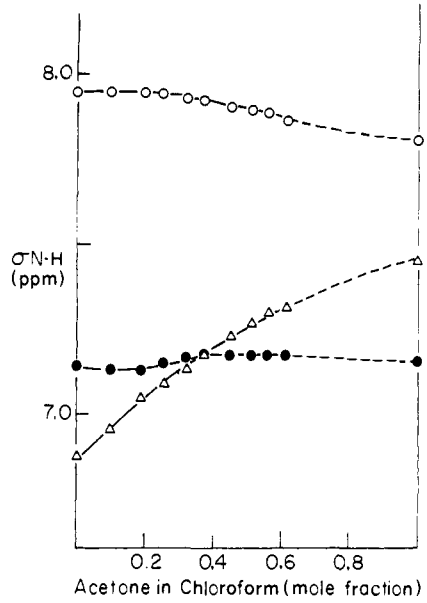

Figure 2. The chemical shift dependence of the amide protons of free PVAV as a function of the mole fraction of acetone in chloroform (-O-, D-Val; -●-, L-Val; -Δ-, D-Ala).

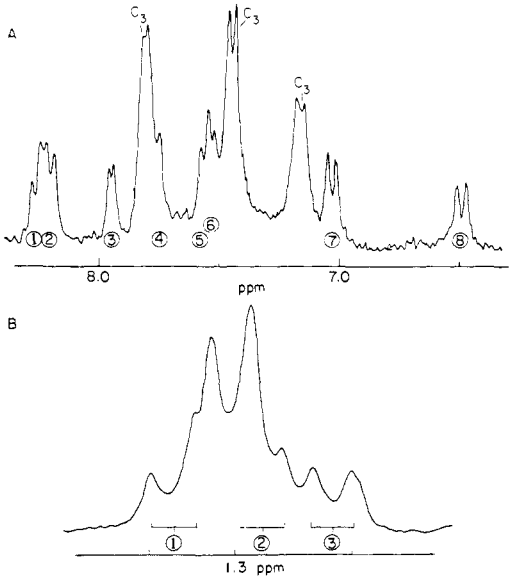

Figure 3. Portions of the ^1H NMR spectra of free PVAV in acetone. (A) Amide region. Lines labeled C_3 are assigned to the C_3-symmetric conformer (see Figure 2). Lines labeled 1-8 are assigned to the asymmetric conformer. The ninth line is under the C_3 peak at 7.45 ppm. (B) Alanine $C_\beta H_3$ lines. The doublets labeled 1, 2, and 3 are assigned to the asymmetric conformer.

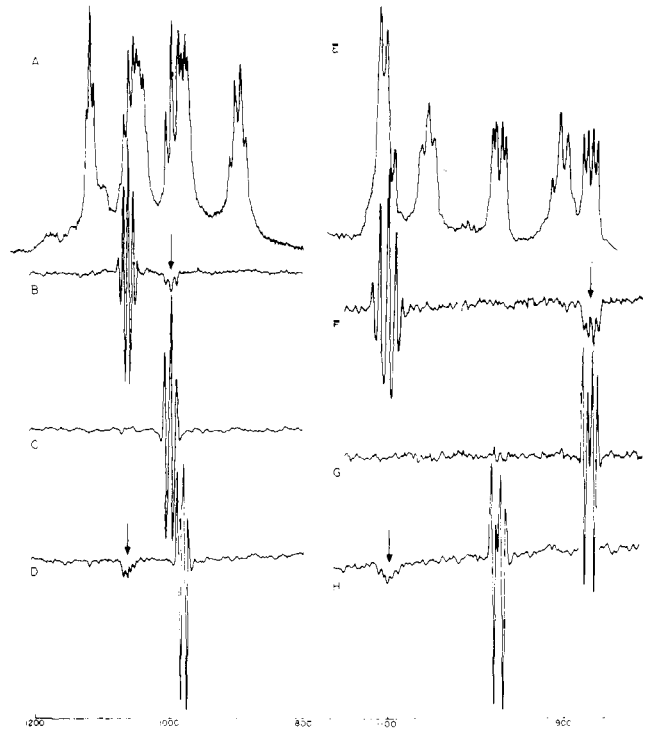

Figure 4. Double resonance difference spectra (250 MHz) of PVAV and K^+-PVAV (C_α-H region). (A) Unperturbed (coupled) spectrum of uncomplexed PVAV. (B) Difference spectrum (coupled minus decoupled) obtained by irradiation of the D-Ala NH at 1718 Hz. (C) Difference spectrum obtained by irradiation of the L-Val NH at 1781 Hz. (D) Difference spectrum obtained by irradiation of the D-valine NH at 1993 Hz. (E) Unperturbed spectrum of K^+-PVAV. (F)-(H): Same sequence as (B)-(D) except irradiations are applied at 1647 (F), 2010 (G), and 2088 Hz (H). Protons showing intensity above and below the base line of the difference spectra are those spin coupled to the irradiated proton; those showing intensity only on the negative (decoupled) side of the base line (arrows) are dipolar coupled to the irradiated proton and experience *positive* NOEs.

Figure 4G) and at 1994 Hz (free PVAV, Figure 4C). There are no detectable NOEs when the high-field N^{Val}-H lines are irradiated (Figures 4D,H).

In principle, Overhauser enhancement factors can be used to calculate absolute internuclear distances. However, this is not possible for molecules the size of PVAV unless the molecular tumbling rate, τ_c^{-1} (ca. 250 MHz), is known exactly.[31-33] Nevertheless, relative distances may be estimated to assign unambiguously which of the lines in Figure 4 correspond to the D and L isomers of valine.

For example, examination of the covalent structure or a molecular model of PVAV shows that the C_α proton which is closest but not spin coupled to the alanine amide proton is that of L-valine; likewise for the L-valine NH, it is the C_α^{Pro}-H; and for the D-valine NH, it is the C_α^{Ala}-H. Moreover, if the peptide bond to N^{Ala}-H is oriented as shown in Figure 6B, the internuclear distance between the N^{Ala} and $C_\alpha^{D\text{-}Val}$ protons is ca. 2 Å, while that between the $N^{L\text{-}Val}$ and C_α^{Pro} protons and the $N^{D\text{-}Val}$ and C_α^{Ala} protons is ca. 3 Å. If the peptide group containing the N^{Ala} were rotated 180° in the opposite direction, all three distances would be approximately the same: 3 Å.

Given this array of internuclear distances, one would predict that the line corresponding to the C_α proton of D-valine would show the greatest Overhauser enhancement upon irradiation of the alanine N-H. Similar considerations apply to the other pairs as well. Accordingly, the lines at 866 (K^+-PVAV, Figure 4F) and at 1000 Hz (PVAV, Figure 4B) can be assigned to the L isomer of valine. The results depicted in Figures 4C and 4G confirm this assignment; irradiation of the low-field valine NH lines give enhancements to the C_α^{Ala}-H lines and therefore must belong to the amide protons of the D isomer. The enhancement factors for the $C_\alpha^{D\text{-}Val}$ lines are greater than those for the C_α^{Ala} lines in both K^+-PVAV and PVAV, as expected for the orientation of the O=C—N^{Ala} group shown in Figure 6B.

D. Cation-Peptide Dissociation. An attempt was made to determine the cation dissociation rate of the K^+-PVAV complex using a line-shape analysis method like the one previously applied to K^+-VAL complexes.[10] This approach, however, was not successful because the dissociation rate for K^+-PVAV is too slow. However, an indirect measurement of the dissociation rate was possible owing to the large differences in the rates of ^2H exchange for the amide protons of K^+-PVAV and free PVAV in methanol-d_4.

Indeed, for the appropriate conditions, it can be shown (see Appendix) that the time dependence for the concentrations of K^+-PVAV ($[KPH_i]$) and free PVAV ($[PH_i]$), each protonated in the ith amide positions and *mixed* 1:1 at time $t = 0$ in methanol-d_4, is given by the equations

$$[KPH_i] = C_{i1}^{+}e^{\lambda_i^{+}t} + C_{i1}^{-}e^{\lambda_i^{+}t} \quad (1)$$

$$[PH_i] = C_{i2}^{+}e^{\lambda_i^{+}t} + C_{i2}^{-}e^{\lambda_i^{+}t} \quad (2)$$

where

$$\lambda_i^{\pm} = -0.5(2k_d + k_{ie}) \pm 0.5(4k_d^2 + k_{ie}^2)^{1/2}$$

In the above, k_d is the rate constant for the dissociation of the cation complex and k_{ie} is the pseudo-first-order rate constant for the exchange of the ith amide proton of the free peptide with deuterated solvent. The coefficients $C_{i1}^{\pm}$ and $C_{i2}^{\pm}$ depend upon the initial conditions. For $[KP^1H_i]_0 = [P^2H_i]_0$:

$$C_{i1}^{+} = [KP^1H_i]_0(k_d + k_{ie} - \lambda_i^{+})/(\lambda_i^{+} - \lambda_i^{+})$$

$$C_{i1}^{-} = [KP^1H_i]_0 - C_{i1}^{+}$$

and

$$C_{i2}^{+} = [KP^1H]_0(k_d/(\lambda_i^{+} - \lambda_i^{-})$$

$$= C_{i2}^{-}$$

As explained in the Appendix, eq 1 and 2 apply under the following conditions. First, the rate of ^2H exchange for the complex, k_{ex}^{MP}, must be much smaller than that for the free form, k_{ex}^{MP}, and, second, the dissociation rate k_d be much less than the association rate k_a (or equivalently that $K_{eq} = [M^+\text{-}P]/[P][M^+] \gg 1$). Although these conditions would be somewhat restrictive in general, they are easily met by K^+-PVAV since k_{ex}^{KP} is on the order of $(\text{days})^{-1}$ and $K_{eq} \geq 10^6$ M.

Analysis of the data shown in Figure 5 reveals that the exchange rates for the D-valine and L-valine amide protons can be classified as "fast" ($k_e^{D\text{-}Val} \gg k_d$) and "slow" ($k_e^{L\text{-}Val} \leq k_d$), respectively. As a result of this, the rate of decay of the D-valine N-H resonance of the complex is essentially the rate of cation dissociation. For $k_{ie} \gg k_d$ and i = D-Val, eq 1 and 2 reduce to

$$[KPH_i] = [KPH_i]_0\exp(-k_d t)$$

$$[PH_i] \simeq 0$$

On the other hand, the rate of decay of the L-Val N-H resonance depends upon both k_d and $k_e^{L\text{-}Val}$. Generalized least-squares fitting[35] of eq 1 and 2 to the data give for the D-Val site, a dissociation rate constant $k_d = 0.026$ (± 0.001) min^{-1}, and a limit of $k_e^{D\text{-}Val} > 0.6$ min^{-1} for exchange. For the L-valine site, the least-squares fit gives a value of 0.019 (± 0.003) min^{-1} for k_d and a value of 0.028 (± 0.002) for $k_e^{L\text{-}Val}$.[36]

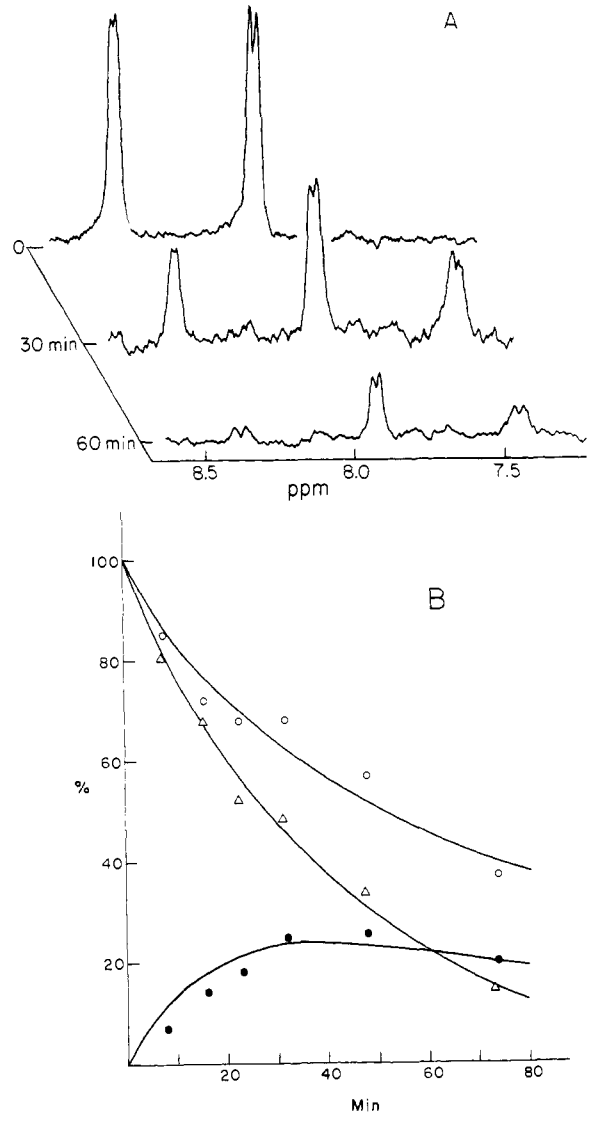

Figure 5. Deuterium exchange of the D-valine and L-valine amide protons in a 1:1 mixture of K^+-PVAV (^1H) and PVAV (^2H) in methanol-d_4. Total peptide concentration is ca. 2×10^{-3} M. The data acquisition times were ca. 1.5 min per spectrum. (A) Amide proton resonances at times $t = 0$, 30, and 60 min after mixing K^+-PVAV (^1H) and PVAV (^2H). (B) Theoretical curves derived from the generalized least-squares fit of eq 1 and 2 (see text). Experimental values are the intensities of the amide protons (-Δ-, $N^{D\text{-}Val}H$ (K^+-PVAV), -○-, $N^{L\text{-}Val}H$ (K^+-PVAV); -●-, $N^{D\text{-}Val}H$ (PVAV)) measured relative to the intensities of the nonexchanging C_α and C_δ protons.

Discussion

A. Three-Dimensional Structure of Complexed and Free PVAV. Comparison of the structural data for the cation complexes of VAL[7,37] and PV[23,38] with those for PVAV reveals several features that are common to all three compounds. These include intramolecular H bonding of the valyl N-Hs, approximate S_6 symmetry for the peptide backbone, and torsional angles $|\phi^{Val}|$ in the range of 60-70°, as well as ligands for cation binding. It is proposed, therefore, that the cation complexes of PVAV also have a bracelet-like shape such that the peptide ring is centered about the cation and is folded into six type II $\beta(1\leftarrow4)$ turns[39,40] as depicted in Figures 6A-C.

This structure is also supported by other data. Both the calculated torsional angle, ϕ_3^{Ala}, and the results of the NOE experiments are consistent with the orientation of the L-Val-D-Ala segment shown in Figure 6B. Furthermore, it has been shown[41] that an axial orientation of the valyl side chains in position 3 of a β turn requires a trans orientation of the $C_\alpha H$ and $C_\beta H$ bonds, and this is observed here.

The conformation of PVAV differs from those of PV and VAL in two distinct ways. For one, the angle $\phi^{L\text{-}Val}$ depends upon the size of the cation. In contrast, in PV and VAL these angles do not show such a dependence. Secondly, the peptide backbone of the PVAV complexes lacks the strict inversion symmetry found in PV and VAL complexes. Thus, the coordination of the cation is not octahedral. As discussed below, the proposed mechanism for cation release and binding may be a consequence of this distortion.

If the cation is removed from the peptide to give free PVAV, the conformation depicted schematically in Figure 6C is no longer the most stable one. This is because the repulsive, dipolar interactions among the inwardly directed carbonyl groups of the valyl residues are no longer offset by attractive, cation-dipole interactions. These repulsive interactions can

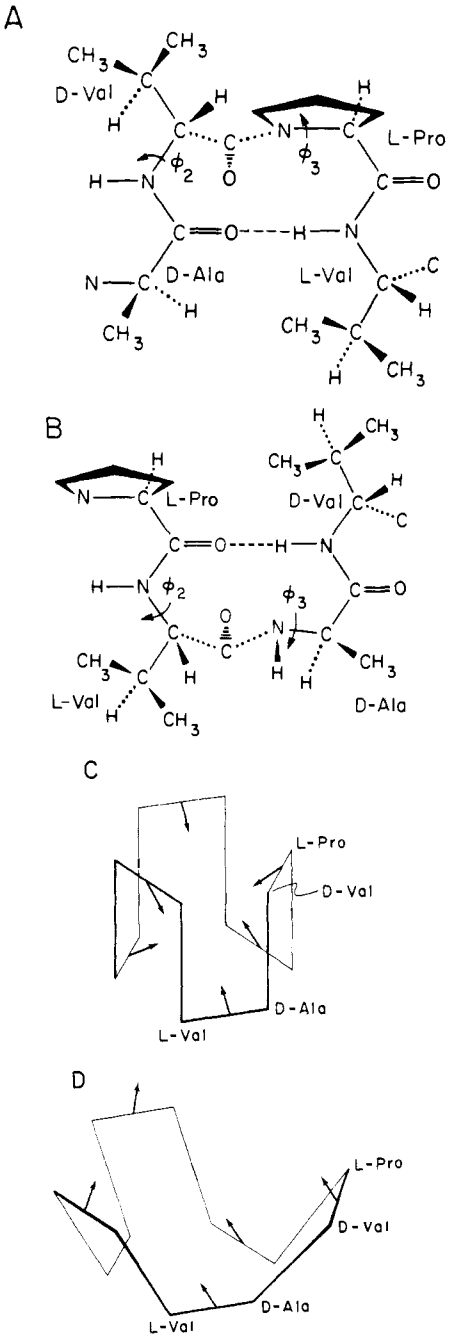

Figure 6. Proposed conformation (type II β (1←4) turns) for the peptide moiety of K^+-PVAV. (A) D-Ala-D-Val-L-Pro-L-Val segment. (B) L-Pro-L-Val-D-Ala-D-Val segment. (C and D) Schematic representations of the peptide backbone configurations in the bracelet (C) and basket (D) conformations. The C_α atoms of the amino acids are located at the corners and the arrows represent the carbonyl ligands of the D- and L-valine residues.

be reduced, however, by conformational changes which lead to an unfolding of the bracelet into a basket (Figure 6D). Owing to the greater freedom of rotation in the $C_\alpha^{L\text{-Val}}$–$C_\alpha^{D\text{-Ala}}$ segment (I) compared to the $C_\alpha^{D\text{-Val}}$–$C_\alpha^{L\text{-Pro}}$ segment (II) the

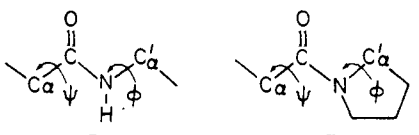

I II

bracelet would be expected to open most easily from the L-Pro side. This change in conformation does in fact occur. In nonpolar solvents, the torsional angle $\phi^{L\text{-Val}}$ increases by 22°, the inversion symmetry is lost, and the hydrogen bonds that stabilize the β turns formed by the L-Pro-L-Val-D-Ala-D-Val segments are weakened if not broken. On the other hand, the β turns formed by the D-Ala-D-Val-L-Pro-L-Val segments remain intact. Moreover, the changes in the other torsional angles as well as the results of the NOE experiments (which indicate an increased separation between the $C_\alpha^{L\text{-Val}}$ and $N^{D\text{-Ala}}$ protons) also support this model.

The observed unfolding of the peptide from the D-Pro, D-Val side suggests a likely pathway for cation capture and release. For in the resulting basket conformation (Figure 6D) the carbonyl groups (arrows) are accessible to uncomplexed cations. Upon capture of a cation the positive charge reorients the carbonyl groups and causes the backbone to fold into the bracelet conformation (Figure 6C). Concomitantly, the disrupted hydrogen bonds re-form and contribute to the stability of the complex.

This mechanism is supported by the results of the kinetic studies which show that, when a cation is released, the D-valine amide protons exchange at least 20 times faster than the L-valine amide protons. (It is generally assumed that free amide protons exchange faster than hydrogen-bonded ones.[27]) It appears therefore that cations leave the peptide such that the hydrogen bonds to the D-Val NH are broken. It is concluded that the preferred pathway for a cation to enter and exit the binding site is through the "top" (proline side) of the molecule.

B. Correlations of Structure and Function. The relative values for the cation affinities of PVAV, PV, and VAL may be understood in terms of the free-energy differences between the complexed and free forms of these molecules. Since the dipole moments of amide ligands are at least twice as large as those of ester ligands[42] and since the cation complexes of PVAV, PV, and VAL are nearly isostructural, it follows on electrostatic grounds that both the PVAV and the PV complexes should be more stable than VAL complexes. By the same reasoning, the free forms of PVAV and PV, were they to retain the bracelet conformation, would be less stable than free VAL, owing to greater repulsive interactions among the free amide dipoles. Thus the net energy gained by cation complexation, and hence the cation affinity, is generally larger for the peptides because, relative to VAL, the complexed states are more stable and the free states are less stable.

Clearly this argument is oversimplified. For one, the cation affinities of PVAV are closer to those of VAL than PV.[18] Secondly, it ignores conformational changes which may occur in the free forms to reduce the repulsive dipolar interactions among the free ligands. The energy reduction gained by these changes depends, however, on whether the carbonyl groups can reorient without disrupting intramolecular hydrogen bonds and without creating strain in other portions of the molecule. In fact, the degree and type of conformational change that occurs upon cation dissociation can be used to gauge how loosely the carbonyl group reorientation is coupled to the rest of the molecular framework.

In VAL the six ester ligands have sufficient rotational freedom so that upon dissociation no significant conformational change occurs in the rest of the backbone.[10] At the other extreme, rotation of the six amide ligands of PV is restricted owing to their linkage to the proline rings. Upon release of the cation, the reorientation of these amide groups forces the peptide backbone into an asymmetric conformation, accompanied by a breaking of hydrogen bonds. However, since the observed concentration ratio of the asymmetric and S_6-symmetric forms of free PV at equilibrium is ca. 3,[23] it is concluded that this reorientation does not add much to the overall stability of the free form.

Between these two extremes stands PVAV. When the cation is lost, the conformation changes from a pseudo-S_6 form to a

C_3-symmetric form. However, the rotational freedom of the amide groups that link the L-Val and D-Ala residues (cf. I and II) permits retention of three of the six hydrogen bonds that stabilize the β turns. Along with this change, all six amide ligands become more favorably oriented (cf. Figures 6C,D).

It appears therefore that the free form of PVAV can achieve some stability via a conformational change that is not accessible to PV. Consequently, the energy change for PVAV-cation complexation would be intermediate between those for PV and VAL, thus placing its affinity for cations in the relative order PV > PVAV > VAL.

The fact that PVAV has a lower affinity for cations than PV does not by itself account for the inactivity of PVAV in bilayer membranes. Indeed, the standard for comparison, VAL, has an even lower affinity for cations. However, the cation dissociation rate for PVAV (as found here) is ca. 10^7 times slower than for VAL.[43] This is significant for it provides experimental support of the proposal that PVAV does not function efficiently as a membrane-bound ion carrier because of its slow dissociation kinetics.[18] One other reasonable pathway for membrane transport is via the solution-complexation mechanism as found for PV.[19] For this pathway to be significant, however, the ion carrier must have a large cation-binding constant in the aqueous phase and such is not the case for PVAV. Thus, both the slow dissociation kinetics and the reduced cation affinity render PVAV inactive as a membrane ion carrier.

Acknowledgments. This work was supported by National Institutes of Health Grants GM 24267 (D.G.D) and GM 24047 (B.F.G). The NMR facilities used are supported by NSF Grant BMS 74-12247 (The Rockefeller University) and NIH Grant RR 00292 (Carnegie-Mellon University). We also wish to acknowledge the assistance of Dr. Stephen Z. Goldberg in the numerical analysis of the kinetic data.

Appendix

In order to derive eq 1 and 2 which govern the ^2H exchange of amide protons in K^+-PVAV-PVAV mixtures, the following reactions must be considered:

$$K^+\text{-PVAV}(^1H_i) + MeO^2H \xrightarrow{k_{ex}^{MPH_i}} K^+\text{-PVAV}(^2H_i) + MeO^1H \quad (1A)$$

$$K^+\text{-PVAV}(^1H_i) \xrightarrow{k_d} PVAV(^1H_i) + K^+ \quad (2A)$$

$$PVAV(^1H_i) + MeO^2H \xrightarrow{k_{ex}^{PH_i}} PVAV(^2H_i) + MeO^1H \quad (3A)$$

$$PVAV(^1H_i) + K^+ \xrightarrow{k_a} K^+\text{-PVAV}(^1H_i) \quad (4A)$$

A separate set of such reactions can be written for each exchangeable proton site (e.g., $N^{D\text{-}Val}H$, etc.). They yield the following rate equations:

$$d[KPH_i]/dt = -k_d[KPH_i] + k_a[PH_i][K^+] - k_{ex}^{MPH_i}[D][KPH_i] \quad (5A)$$

$$d[PH_i]/dt = -k_{ex}^{P_i}[D][PH_i] - k_a[PH_i][K^+] + k_d[KPH_i] \quad (6A)$$

where $[KPVAV^1H_i] = [KPH_i]$, $[MeO^2H] = [D]$, etc.

Case I. If only K^+-PVAV is present, then

$$[K^+] = [PH_i] \text{ and}$$

$$[KPH_i] = K_{eq}[PH_i][K^+] \quad (7A)$$

where K_{eq} is the equilibrium constant for association. Substituting the right-hand side of (7A) for the quantity $[KPH_i]$ in (5A) and expressing K_{eq} in terms of the rate constants, k_a and k_d (i.e., $K_{eq} = k_a/k_d$), leads to the cancellation of the first two terms in (5A) and gives

$$d[KPH_i]/dt = -k_{ex}^{MP}[D][KPH_i]$$

or, integrating

$$[KPH_i] = [KPH_i]_0 \exp(-k_{ex}^{MP_i}[D]t)$$

Experimentally it is found that $k_{ex}^{MPH_i}$ is on the order of (several days)$^{-1}$. In other words the rate of exchange of amide protons with solvent in K^+-PVAV is much smaller than the other rate constants appearing in eq 5A and 6A and may be ignored in the subsequent analysis.

Case II. If, in addition to K^+-PVAV, a finite amount of free PVAV is also added to the reaction mixture in methanol-d_4 such that $[KP]_0 = [KPH] + [KPD]$, and $[P]_0 = [PH] + [PD]$, then

$$[K^+] = \alpha = K_{eq}^{-1}([KP]_0 - \alpha)/([P]_0 + \alpha)$$

Since $\alpha \ll [KP]_0$ and $[P]_0$

$$[K^+] = K_{eq}^{-1}[KP]_0/[P]_0 = (k_d/k_a)[KP]_0/[P]_0 \quad (8A)$$

If $[KP]_0 = [P]_0$, then according to (8A) $[K^+] = k_d/d_a$. With the substitution of this expression for $[K^+]$ into (5A) and (6A) they reduce to

$$d[KPH_i]/dt = -(k_d + k_{ex}^{MPH_i}[D])[KPH_i] + k_d[PH_i] \quad (9A)$$

$$d[PH_i]/dt = -(k_{ex}^{P_i}[D] + k_d)[PH_i] + k_a[KPH_i] \quad (10A)$$

Equations 9A and 10A represent a system of coupled first-order differential equations which can be solved by standard methods.

References and Notes

(1) (a) Adelphi University. (b) The Rockefeller University.
(2) Brockmann, H.; Schmidt-Kastner, G. *Chem. Ber.* **1955**, *88*, 57–61.
(3) Shemyakin, M. M.; Aldanova, N. A.; Vinogradova, E. I.; Feigina, M.Yu. *Tetrahedron Lett.* **1963**, *28*, 1921–1925.
(4) Moore, C.; Pressman, B. C. *Biochem. Biophys. Res. Commun.* **1964**, *15*, 562–567.
(5) Lev, A. A.; Buzhinsky, E. P. *Tsitologiya* **1967**, *9*, 102–106.
(6) For a review see Ovchinnikov, Yu. A.; Ivanov, V. T.; Shkrob, A. M. "Membrane-Active Complexones", Elsevier: Amsterdam, 1974.
(7) Pinkerton, M.; Steinrauf, L. K.; Dawkins, P. *Biochem. Biophys. Res. Commun.* **1969**, *35*, 512–518.
(8) Ivanov, V. T.; Laine, I. A.; Abdulaev, N. D.; Senyavina, L. B.; Popov, E. M.; Ovchinnikow, Yu. A.; Shemyakin, M. M. *Biochem. Biophys. Res. Commun.* **1969**, *34*, 803–811.
(9a) Urry, D. W.; Ohnishi, M. In "Spectroscopic Approaches to Biomolecular Conformation", Urry, D. W., Ed.; American Medical Association: Chicago, 1970; pp 263–400.
(9b) Patel, D. J.; Tonelli, A. E. *Biochemistry* **1973**, *12*, 486–496.
(10) Davis, D. G.; Tosteson, D. C. *Biochemistry* **1975**, *14*, 3962–3969.
(11) Shemyakin, M. M.; Ovchinnikov, Yu. A.; Ivanov, V. T.; Antonov, V. K.; Vinogradova, E. I.; Shkrob, A. M.; Malenkov, G. G.; Evstratov, A. V.; Laine, I. A.; Melnik, E. I.; Ryabova, I. D. *J. Membr. Biol.* **1969**, *1*, 402–430.
(12) Merrifield, R. B.; Gisin, B. F.; Tosteson, D. C.; Tieffenberg, M. In "The Molecular Basis of Membrane Function", Tosteson, D. C., Ed.; Prentice-Hall: Englewood Cliffs, N.J., 1969; pp 211–220.
(13) Gisin, B. F.; Merrifield, R. B. *J. Am. Chem. Soc.* **1972**, *94*, 6165–6170.
(14) Urry, D. W.; Cunningham, W. D.; Ohnishi, T. *Biochim. Biophys. Acta* **1973**, *292*, 853–857.
(15) Baron, D.; Pease, L. G.; Blout, E. R. *J. Am. Chem. Soc.* **1977**, *99*, 8299–8306.
(16) Hollósi, M.; Wieland, T. *Int. J. Pept. Protein Res.* **1977**, *10*, 329–341.
(17) Ting-Beall, H. P.; Tosteson, M. T.; Gisin, B. F.; Tosteson, D. C. *J. Gen. Physiol.* **1974**, *63*, 492–508.
(18) Gisin, B. F.; Ting-Beall, H. P.; Davis, D. G.; Grell, E.; Tosteson, D. C. *Biochim. Biophys. Acta* **1978**, *509*, 201–217.
(19) Benz, R.; Gisin, B. F.; Ting-Beall, H. P.; Tosteson, D. C.; Lauger, P. *Biochim. Biophys. Acta* **1976**, *455*, 655–684.
(20) Stark, G.; Benz, R. *J. Membr. Biol.* **1970**, *5*, 133–153.
(21) Dadok, J.; Sprecher, R. F.; Bothner-By, A. A.; Link, T. Proceedings of the 11th Experimental NMR Conference, Pittsburgh, Pa., 1970.
(22) Dadok, J.; Sprecher, R. F. *J. Magn. Reson.* **1974**, 243–248.
(23) Davis, D. G.; Gisin, B. F.; Tosteson, D. C. *Biochemistry* **1976**, *15*, 768–774.
(24) Ramsey, N. F. *Phys. Rev.* **1955**, *100*, 1191–1194.
(25) Solomon, I. *Phys. Rev.* **1955**, *99*, 559–565.
(26) Noggle, J. H.; Schirmer, R. E. "The Nuclear Overhauser Effect", Academic Press: New York, 1971.
(27) Craig, L. C.; Cowburn, D.; Bleich, H. *Annu. Rev. Biochem.* **1975**, *44*, 477–490.

(28) (a) Judging from the line widths at 23 °C, the asymmetric conformer does not interconvert with itself or with the C_3-symmetric conformer a rate ≥ 1 s^{-1}. At 40 °C the lines of the asymmetric conformer but not those of the C_3-symmetric conformer begin to broaden. This indicates that the rate of *intra*molecular conversion is faster than that of *inter*molecular conversion. (b) See, e.g., Pople, J. A.; Schneider, W. G.; Bernstein, H. J. "High-Resolution Nuclear Magnetic Resonance", McGraw-Hill: New York, 1959; Chapter 10.
(29) Bystrov, V. F. *Prog. Nucl. Magn. Reson. Spectrosc.* **1976**, *10*, 41–81.
(30) Ramachandran, G. N.; Chandrasekaran, R.; Kopple, K. D. *Biopolymers* **1971**, *10*, 2113–2131.
(31) Balaram, P.; Bothner-By, A. A.; Dadok, J. *J. Am. Chem. Soc.* **1972**, *94*, 4015–4016.
(32) Glickson, J. D.; Gordon, S. L.; Pitner, T. P.; Agresti, D. G.; Walter, R. *Biochemistry* **1976**, *15*, 5721–5729.
(33) When $\tau_c\omega_0 \sim 1$, the sign and magnitude of $f_A(B)$ (hence the calculated intermolecular distances) depend critically on the exact value of $\tau_c\omega_0$.[31,32] This is illustrated by the fact, at $\omega_0/2\pi = 250$ MHz, the NOEs for VAL in Me_2SO are negative[32] whereas in chloroform they are positive, not only for VAL but also K^+-VAL (Davis, D. G. Unpublished, 1977).
(34) Since k_d (the dissociation rate constant) $\sim \tau^{-1}$ (the average lifetime of the complex) $\ll T_2^{-1} = 2\pi\Delta\nu_{1/2}$ (the natural line width) no line broadening due to dissociation can be observed. See ref 28b.
(35) Busing, W. R.; Levy, H. A. "OR GLS, a General Fortran Least Squares Program", ORNL-TM-271, 1962.
(36) The rate of isotope exchange for free PVAV can be measured separately, giving values of ≥ 0.4 and 0.04 (± 0.005) min^{-1} for $k_e^{D\text{-}Val}$ and $k_e^{L\text{-}Val}$, respectively.
(37) Neupert-Laves, K.; Dobler, M. *Helv. Chim. Acta* **1975**, *58*, 432–442.
(38) Hamilton, J. A.; Sabesan, M. N.; Gisin, B. F.; Steinrauf, L. K. *Biochem. Biophys. Res. Commun.* **1978**, *80*, 949–954.
(39) Venkatachalam, G. N. *Biopolymers* **1968**, *6*, 1425–1436.
(40) Chandrasekaran, R.; Lakshinarayanan, A. V.; Pandy, U. V.; Ramachandran, G. N. *Biochim. Biophys. Acta* **1973**, *303*, 14–27.
(41) Mayers, D. F.; Urry, D. W. *J. Am. Chem. Soc.* **1972**, *94*, 77–81.
(42) McClellan, A. L. "Tables of Experimental Dipole Moments", W. H. Freeman: San Francisco, 1963.
(43) Funck, Th.; Eggers, F.; Grell, E. *Chimia* **1972**, *26*, 637–641.
(44) IUPAC–IUB Commission on Biochemical Nomenclature. *J. Mol. Biol.* **1970**, *52*, 1–17.
(45) Pachler, K. G. R. *Spectrochim. Acta* **1974**, *20*, 581–587.
(46) Although there are four possible torsional angles for a given vicinal coupling constant, molecular models which incorporate the symmetry features, the H-bonding patterns, and the ion-binding requirements as well as the results of the NOE experiments for these molecules indicate that only the values given in Table II are physically realistic.

Barriers to Rotation of Methyl Groups in 9-Methyltriptycene and 9-Methyl-9,10-dihydro-9,10-ethenoanthracene

Fumio Imashiro, Takehiko Terao, and A. Saika*

Contribution from the Department of Chemistry, Kyoto University, Kyoto 606, Japan. *Received September 20, 1978*

Abstract: Rotational barriers of methyl groups in solid 9-methyltriptycene (**1**) and 9-methyl-9,10-dihydro-9,10-ethenoanthracene (**2**) are determined to be 5.16 ± 0.10 and 3.35 ± 0.04 kcal/mol for **1** and **2**, respectively, by the temperature dependence of the ^1H spin–lattice relaxation times. Calculations of the rotational barriers by the molecular mechanics (MM1) method give too large values, while those by the molecular orbital (CNDO/2) method yield reasonable values. The diminution of the rotational barriers by the CNDO/2 method can be interpreted by nonbonded attractive interactions between the unoccupied σ^*_{CH} orbitals of the methyl group and the occupied σ_{CH} orbitals of the peri CH bonds in the rotational transition state.

Since 9-methyltriptycenes are considered to have intramolecularly large steric hindrances about the methyl groups due to substituents at peri positions and consequently to have large barriers to methyl rotation, DNMR studies in solutions have been carried out by Öki et al.[1,2] on several peri-substituted 9-methyltriptycenes to investigate their rotational barriers. However, the barrier of the most interesting and fundamental compound, 9-methyltriptycene (**1**) itself, cannot be measured by the DNMR method because of its molecular symmetry.

In this article the authors have measured the ^1H spin–lattice relaxation times (T_1) in the solid state of **1** and 9-methyl-9,10-dihydro-9,10-ethenoanthracene (**2**) (Figure 1) having less steric hindrance due to fewer peri hydrogens, and have determined the barriers to rotation of the methyl groups of **1** and **2** from the temperature dependence of T_1 values. Relaxation mechanisms for **1** and **2** seem to be much simpler in solids than in solutions, because in solids the molecular motion efficient for the relaxation is expected to be only the methyl rotation whereas molecular tumbling and molecular diffusion are also important relaxation mechanisms in solutions.[3]

Further, the origin of the rotational barriers for **1** and **2** is considered on the basis of molecular mechanical calculations (the MM1 method[4]) and molecular orbital calculations (the CNDO/2 method[5]), and an interesting result is found that in addition to the "steric effects" nonbonded attractive interactions[6] between the methyl group and the peri group notably influence the rotational barrier.

Experimental Section

Materials. Melting points were uncorrected. Mass, infrared, and NMR spectra were recorded on Hitachi RMU-6C mass, JASCO IRA-1 diffraction grating infrared, and Varian HA-100 spectrometers, respectively.

A. 9-Methyltriptycene (1). **1** was prepared by treating 9-methylanthracene with benzyne in the manner similar to the preparation of 1,4,9-trimethyltriptycene.[2] Purifications through a silica gel column and by repeated recrystallizations gave **1** as colorless prisms, mp 270 °C (lit. 253–254,[7] 258–259 °C[8]).

B. 9-Methyl-9,10-dihydro-9,10-ethenoanthracene (2). In a sealed glass tube a mixture of 0.8 g of 9-methylanthracene and 4.2 g of *trans*-dichloroethylene was heated for 24 h at 200 °C. After cooling, the sealed tube was opened and the reaction mixture was chromatographed on a silica gel column eluted with CCl_4. The eluate was concentrated, and the residue was refluxed with a mixture of 5 g of Zn, 150 mg of $CuSO_4$, 1 mL of water, and 20 mL of ethanol for 4 h. After cooling, the whole was extracted with ether and the extract was washed with aqueous NaCl and dried over anhydrous Na_2SO_4. The solvent was evaporated, and the residual white solids were chromatographed on a silica gel column. The fraction eluted with benzene–hexane (2:1) was concentrated, and the residual crystals were recrystallized with petroleum ether to give 670 mg (74%) of **2** as colorless prisms: mp 98.0–98.5 °C; NMR δ (CCl_4) 2.12 (3 H, s, methyl), 4.97 (1 H, dd, J = 6.0, 1.5 Hz, bridgehead), 6.50 (1 H, dd, J = 7.0, 6.0 Hz, olefinic), 6.80–6.92 (4 H, m, aromatic), 6.95 (1 H, dd, J = 7.0, 1.5 Hz, olefinic), 7.08–7.26 (4 H, m, aromatic); IR (cm^{-1}) 1445, 1330, 1020, 760, 740, 680; mass spectrum *m/e* (rel intensity) 218 (M^+, 57), 203 (100), 202 (42). Anal. ($C_{17}H_{14}$) C, H.

Measurements. Samples for NMR measurements were degassed by several freeze–pump–thaw cycles. Measurements of T_1 were performed using a homemade pulsed spectrometer operated at 59.5 MHz. T_1 values were determined by the saturation–recovery method; ten 90° pulses at 1.2-ms intervals were applied for saturation,[9] and the solid-echo method[10] was used in order to detect full FID amplitudes hidden by the dead time. A least-squares analysis of the data points enabled T_1 to be determined within an error of ±5%. Tem-

0002-7863/79/1501-3762$01.00/0